BONE FRACTURES UNDER THE MICROSCOPE

An Experimental Approach to Mid-Upper Paleolithic Faunal Remains

Soňa Boriová [ID] – **Alan K. Outram** [ID] – **Zuzana Pokorná** [ID] – **Sandra Sázelová** [ID]

Bone fragmentation results from different natural processes or various activities employed by several taphonomic agents. However, it may also represent direct evidence of deliberate human activity connected to the exploitation of animal resources throughout the Paleolithic period. Extensive long mammal bone fragmentation research resulted in last decades into description of individual fracture characteristics reflecting the background of fragmentation process (*Johnson 1985*; *Outram 2001*). The features combine macroscopic traits such as angle, an outline, and surface texture of the fracture. However, as the experimental works show, the response of bone on a gross scale is in great extent given by microstructure and its state of preservation directly correlating with the biomechanical properties (*Currey 2012*; *Gifford-Gonzales 2018*). The paper aims on testing (1) whether the microscopic features correlate with described macro-scale differences or even (2) are able to distinguish features with macroscopic overlaps but of different origin. We have thus tested and applied two microscopic methods on two experimental assemblages with documented fragmentation conditions. By the scanning electron microscopy (SEM) we observed irregularities and micro-fractures in bone fracture surface (FS). They proved to be in certain aspect specific for a given state of bone preservation. Transmitted light microscopy mapped the abundance of micro-cracking, its characteristic features in relation to bone preservation and specific way of fragmentation. The histological thin-sections (HTS) revealed a variety of micro-cracking penetrating the FS, but they did not prove any differentiating pattern among observed experimental sets. A range of different surface profiles was documented, the profile morphology seems to be characteristic for individual bone preservation states. If compared to macroscopic method (FFI), the study of microscopic features in their presented extent did not allow us to differentiate further between fractures. Finally, we undertook an example application of the macroscopic fracture analysis on settlement areas from the Gravettian site Pavlov I (Czech Republic) and we discuss the potential of suggested micro-methods in taphonomic analysis dealing with animal body manipulation and exploitation.

INTRODUCTION

Differentiation of human activity from other similar modifications with different origin in archaeozoological assemblages is an important topic not only in case of Early and Middle Paleolithic sites, where we are trying to prove the earliest intentional human intervention as a part of actively ongoing hunting-scavenging and exploitation debates (*Blumenschine 1995*; *Capaldo 1997*; *Domínguez-Rodrigo 2002*; *Domínguez-Rodrigo/Barba 2006*; *Parkinson 2018*). When dealing with Upper Paleolithic settlements, human activities result in various archaeological evidence such as the presence of settlement structures, activity zones, hearths, and various types of artefacts made from organic and inorganic materials. Nevertheless, people are not the only depositional and post-depositional agents who produce and leave their traces at a site. Other taphonomic factors, for example carnivores or different environmental/natural processes, can display equifinality in the traces they leave when compared to human activities and therefore complicate our understanding of the taphonomic history of site formation processes (*Capaldo/Blumenschine 1994*; *Galán et al. 2009*; *Haynes 1983*; *Karr 2012*; *Karr/Outram 2012b*; *Li 2018*; *Stiner 2004*; *Thorson/Guthrie 1984*).

Attention is paid to fragmentation as one of the key features of intentional human modification of mammal long bones, both for nutritional but also utilitarian and symbolic purposes (*Binford 1981*; *Bradfield/Brand 2015*; *Hutson et al. 2018a*; *Johnson 1985*; *Lyman 1994*). Simultaneously, the identification of the

precise actor responsible for fragmentation of bone material, without additional supportive and comparative evidence, presents a delicate issue. There is a significant amount of archaeology-oriented research dealing with fragmentation and its different forms and comparing their characteristics by employing experiments on modern animal bones. Firstly, the research focuses on fracture and its characteristics such as outline, angle or surface texture and their description, evaluation, and proportions in assemblages (e.g. *Alcántara-García et al. 2006*; *Coil/Tappen/Yezzi-Woodley 2017*; *Johnson 1985*; *Moclán/Domínguez-Rodrigo/ Yravedra 2019*; *Morlan 1984*; *Outram 2001*; *Shipman 1981*; *Villa/Mahieu 1991*). The description of fracture features is mainly qualitative and focuses on:

a) the outline (e.g. transverse/helical/longitudinal);
b) the surface texture (smooth/rough);
c) the angle (perpendicular/oblique).

Nevertheless, various approaches considering measurements, proportions, constructing scoring systems and calculating mean values for these characteristics add an additional quantitative aspect (*Marean et al. 2000*; *Merritt/Davis 2017*). Secondly, the research focus on the fragmentation-accompanying traces, usually classified as a bone surface modifications (BSMs), includes for example percussion marks, percussion pits, percussion, impact or rebound notches and percussion flakes. They may result from hammerstone percussion as well as from the carnivore manipulation of bones (*Capaldo/Blumenschine 1994*; *Galán et al. 2009*; *Organista et al. 2016*; *Pickering/Egeland 2006*; *Vettese et al. 2020*). The BSMs appearing alongside fragmentation processes are studied from both quantitative (abundance, measurements, frequencies, proportions of individual traits) and qualitative (shape, presence of striations) aspects. Several systematic differences between human vs. carnivore breakage agents have been successfully described, for example types and quantification of accompanying bone surface modifications (*Galán et al. 2009*; *Thompson et al. 2017*). However, some aspects, for example types and proportion of fracture surface angles (e.g., *Moclán/ Domínguez-Rodrigo/Yravedra 2019*), in differentiation of fragmentation actors remain unsolved and call for deeper analytic and experimental work (*Haynes 1983*; *Haynes/Krasinski/Wojtal 2021*; *Thompson et al. 2019*).

The above-mentioned studies address the bone fragmentation topic in contexts with numerous variables or conditions, which influence the final response of bone to the applied impact observable in archaeological record. For example, state of bone preservation, type of fracturing force, type and size of affected skeletal element, presence of soft tissues, or even human intuitiveness and its role in the process (*Karr 2012*; *Karr/Outram 2012a*; *2012b*; *2012c*; *Pickering/Egeland 2006*; *Tappen 1969*; *Tappen/Peske 1970*; *Vettese et al. 2021*; *Waterhouse 2013*).

The biomechanical properties of the bone in different conditions have a vast impact on the nature of bone fracture and fragmentation. The moisture content and bone preservation also significantly influence the bone viscoelasticity presenting one of the most important features in fracture resistance. Even though these variables may complicate our understanding to regularities observed in fragmentation process, they make bone a uniquely powerful material in understanding taphonomy and site formation processes. If properly documented, analysed, and understood, the changes in the way the bone fractures in response to condition and mode of fracture, may be richly informative. The natural ability of bone to resist impact decreases when the moisture is lost, during process of drying or freezing (*Bonnichsen 1979*; *Johnson 1985*; *Karr/Outram 2012b*; *Stanford/Bonnichsen/Morlan 1981*) and most probably in the opposite extreme too (e.g. *Haglund/Sorg 2002*; *Hedges/Millard 1995*). A stress force applied beyond the plastic limit of bone causes irreversible changes in it, beginning on the micro-scale, and leads to fragmentation on a gross level if not disrupted (*Johnson 1985*). Furthermore, fracture resistance is provided by the anisotropic nature of bone material too. The unique microscopic grading of the bone structure together with the overall shape of the bone lead to specific response to applied stress (*Currey 2012*; *Hamed/Lee/Jasiuk 2010*; *Johnson 1985*; *O´Brien et al. 2005*). The fresh bone reacts more or less uniformly to stress by helical fracture (e.g. *Evans 1957*; *Haynes 1983*; *Johnson 1985*) and it was long believed that this fracture type presents a characteristic trait for human fragmentation. However, the reflection the bone state preservation and amount of applied force seemed to be more plausible options. The topic was further investigated by *P. Shipman* (*1981*) who introduced scanning electron microscopy (SEM) into archaeological bone fracture investigation, describing two types of the helical fracture. Type I (a) is typical by a fracture plane lying in between two adjacent collagen bundles, leading to smooth surface appearance on the microscopic level. This fracture type is caused by any agent capable of achieving helical fracturing by the application of force in a direction identical to the prevalent collagen bundle orientation causing the failure of bonds between neighbouring bundles. Type II (b) is characterised by a rough and stepped surface caused by

perpendicular orientation of the fracture front to the main collagen bundle orientation. The fracture front spreads alongside different laminae and always accompanies each for a short distance, just before it transverses to another. This type of fracture is shared by any agents developing enough torsional force to overcome the structural strength of the bone, except for weathering or trampling (*Shipman 1981*, 371, 372). Of course, these traits may be influenced by the state of bone preservation as the collagen bundles subject to decay and break down. Her study showed the potential in distinguishing of microscopic fracture features, however to our recent knowledge the approach was not further deeply developed.

Other studies showed (*Currey 2002*; *2012*; *Johnson 1985*) that the initial micro-cracking tends to travel into the compact bone in between the bone laminae and follows the osteon structure, which is in the case of long bones predominantly parallel to their long axis. Thus, drying may often in long bones cause longitudinal fractures. In the fresh bone, the micro-fracture originates or tend to be deflected by the cement lines bonding individual osteons and the surrounding bone matrix. The cement line represents a layer with different composition than surrounding bone and does not contain collagen, and therefore represents a place where micro-cracking expands, instead of intersecting through the Haversian system (*Li/Abdel-Wahab/Silberschmidt 2013*; *Rho/Kuhn-Spearing/Zioupos 1998*; *Tang et al. 2015*). Nevertheless, these facts result from material studies, where bone is subjected mainly to static loading in standardized conditions using uniformly shaped bone samples in small blocks (e.g. *Li/Abdel-Wahab/Silberschmidt 2013*; *Wang 2011*; *Zioupos/Kirchner/Peterlik 2020*). Since the overall bone morphology and its size have a significant impact on the final response to fragmentation force (*Blasco et al. 2014*; *Gifford-Gonzales 2018*), the verification of the diagnostic capability in the study of micro-features for the archaeological fragmentation issues, however, cannot be fully held in standardized bone blocks lacking important original bone shape and size variables.

In this study we employed scanning electron microscopy and histological methods for deeper observation of the specific microscopic features on the fracture surface and in the surrounding bone microstructure resulting from the fragmentation process. We examined two experimental assemblages and subject them to the standardized treatment and observation. Our results are compared to the macroscopic evaluation of FFI (*Outram 2001*), and we discuss their potential application for archaeozoological assemblages, based on the example of selected areas from the Mid-Upper Paleolithic site Pavlov I (*Svoboda et al. 2016*).

MATERIAL

The first experimental set (Set 1) subjected to microscopic analyses consists of recent domestic cattle (*Bos taurus*) long bones (*humerus, radio-ulna, femur, tibia*) from individuals aged between 18 to 36 months. The material originates from the rockfall experiments conducted at the University of Exeter (*Karr 2012*) in 2010. Bones were fragmented in three different stages of their preservation, 32 bones were fragmented per each stage:

a) fresh;

b) dried (at 20°C for 20 hours without soft tissues, and for 40 days with soft tissues);

c) frozen (at –20 °C for 15 days) bones with and without residual soft tissues were fragmented by a series of rock falls (2–12 kg) on solid ground (concrete-paved area). The experiment was aimed on assessing occurrence of accidental pseudo-flakes, which could be produced by specific environmental activity in archaeozoological assemblages (for further details see *Karr 2012*; *Karr/Outram 2012a*; *2012b*; *2012c*). We have selected this type of material due to three different states of preservation and repeated dynamic impact of non-human origin.

The second experimental set (Set 2) consists of recent European and fallow deer (*Cervus elaphus et Dama dama*) long bones (*humerus, radio-ulna, femur, tibia*) from four individuals aged between 18 months and 5 years. The experiment was realized at the Research Centre for Paleolithic and Paleoanthropology, Dolní Věstonice, Institute of Archaeology, Brno (IA Brno) in 2020 and 2021. Twelve bones were fragmented when in a fresh state with periosteum still attached to the bone during the fragmentation process. The experiment was designed to model intentional human activity. Six experimenters were instructed to break the bone to open the marrow cavity using an unmodified hammerstone (pebble) and hard flat anvil placed on the solid ground. These samples expanded the fresh bone sample size obtained from the Exeter experiments, representing outcomes of human-derived dynamic loading.

The archaeological material originates from excavations in 2013–2015 at Pavlov I site, namely settlement area SE014 (with units S1, S2 and surrounding area), activity areas A and G (*Svoboda et al. 2016*). The long fore and hind limb bones (*humerus, radio-ulna, metacarpus, femur, tibia, metatarsus*) and their fragments of wolf (*Canis lupus*) and reindeer (*Rangifer tarandus*) were subjected to FFI calculation.

METHODS

Both experimental and archaeological samples were subjected to macroscopic evaluation and calculation of fragmentation freshness index (FFI; *Outram 2001*). This index is based on scoring of three basic fracture characteristics. Each criterion can be scored from 0 for characteristics of fresh fracture, 1 for a mix of fresh and dry bone features, and 2 for characteristics of bone fractured in intensively altered state (Tab. 1). The final score for each specimen can vary from 0 to 6. Score around 3 is ambivalent and can point at mixed fragmentation history (*Johnson/Parmenter/Outram 2016*). The index value is the considered in relation to microscopic observations, to test if any correlation is present or absent, and if microscopic observation can have additional value to FFI determinations. In each experimental set, average FFI value is therefore stated, and complemented by the minimal and maximal score in examined assemblage.

Tab. 1. Scoring of individual criteria necessary in fragmentation freshness index (FFI) calculation (according to *Outram 2001*, 406). Author S. Boriová.

Score	Angle of fracture surface	Fracture surface texture	Fracture surface outline
0	no more than 10% perpendicular to bone surface	entirely smooth	mainly helical breaks
1	between 10% and 50% perpendicular to bone surface	some roughness present, but mainly smooth	mixture of outlines
2	more than 50% perpendicular to bone surface	mainly rough	absence of helical outlines

In the next step, the fracture surfaces of the experimental samples were cut by a hand saw Proxxon FBS 240/E and its diamond disc into the squares with approximately 1 × 1 cm (Fig. 1). The cut samples were then dehydrated in alcohol row (70%, 90%, 96% and 99.8%; in each for 30 min.). We used SEM to study the micro-morphology of the fracture surfaces and thus the samples were coated by chromium (a layer of 55 nm) or chromium and gold (a layer of 20 nm both) by a magnetron sputtering. The fracture surfaces were then analysed by scanning electron microscopes JEOL JSM 6700F and MAGELLAN 400 with Everhart-Thornley and in-lens detector at 5 keV at the Institute of Scientific Instruments, Czech Academy of Sciences in Brno. The general overviews on the entire sample surface were taken at an approximate

Fig. 1. Example of sampling for SEM and histological thin-section preparation. Spiral fracture surface, sample Q, Set 2. Photo S. Boriová.

magnification interval from 35× to 39× (one pixel then corresponds here to 2.85–2.56 μm). The individual images were then merged in one using the Automatic Photomerge routine in Adobe Photoshop.

Finally, to describe possible micro-cracking and edge of the fracture in relation to surrounding bone micro-structure, the histological thin sections (HTS) were prepared. Same samples as for the SEM, were employed in order to provide a better correlation in between our results and to minimize the bone destruction. Preparation process followed the standard protocol (*Sázelová/Boriová/Šáliová 2021*). The thin sections were examined under the optical microscope Leica DM2500 LED with transmitted and polarized light (Leica DMC 6200 microscope camera, LasX software) and captured mainly on an overall magnification 50× (one pixel corresponds to 1.17 μm). The research facilities were provided by the Research Centre for Paleolithic and Paleoanthropology, Dolní Věstonice, IA Brno, Czech Academy of Sciences.
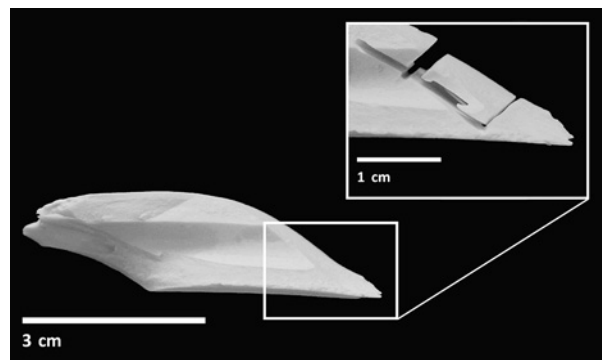
Tab. 2. List of samples analysed by both microscopic methods. Author S. Boriová.

Sample	Experiment	Species	Preservation state	Periost/soft tissues	Fragmentation process	Fracture outline
B	Set1	*Bos taurus*	fresh	present	rockfall	longitudinal
K	Set1	*Bos taurus*	fresh	present	rockfall	helical
L	Set1	*Bos taurus*	fresh	missing	rockfall	longitudinal
N	Set1	*Bos taurus*	fresh	missing	rockfall	helical
C	Set1	*Bos taurus*	frozen	missing	rockfall	longitudinal
D	Set1	*Bos taurus*	frozen	present	rockfall	longituidnal
E	Set1	*Bos taurus*	frozen	present	rockfall	helical
M	Set1	*Bos taurus*	frozen	missing	rockfall	helical
A	Set1	*Bos taurus*	dried	present	rockfall	longitudinal
F	Set1	*Bos taurus*	dried	present	rockfall	transversal/helical
G	Set1	*Bos taurus*	dried	missing	rockfall	longitudinal
J	Set1	*Bos taurus*	dried	missing	rockfall	transversal
O	Set2	*Dama dama*	fresh	present	human	helical
P	Set2	*Cervus elaphus*	fresh	present	human	helical
Q	Set2	*Cervus elaphus*	fresh	present	human	helical
R	Set2	*Cervus elaphus*	fresh	present	human	helical
S	Set2	*Cervus elaphus*	fresh	present	human	longitudinal
T	Set2	*Cervus elaphus*	fresh	present	human	longitudinal
U	Set2	*Cervus elaphus*	fresh	present	human	longitudinal
V	Set2	*Cervus elaphus*	fresh	present	human	longitudinal
W	Set2	*Dama dama*	fresh	present	human	helical
X	Set2	*Dama dama*	fresh	present	human	helical
Y	Set2	*Dama dama*	fresh	present	human	longitudinal
Z	Set2	*Cervus elaphus*	fresh	present	human	longitudinal

In total, 24 experimental samples were subjected to detailed analysis, half of them originated from the Set 1 representing longitudinal, transversal and helical fractures; and the second half came from the Set 2 and covers bones with longitudinal and helical fractures (Tab. 2). Each sample was chosen from diaphysis fragments longer than 4 cm in the longest axis in order to represent each fragmentation category.

RESULTS

Experimental Set 1

In freshly fragmented bones the mean FFI was 2.85. The distribution of individual FFI score is visualized in Fig. 2. The modal FFI score was 2. The SEM examination revealed several common traits for both, longitudinal and helical fractures. The main features are summarised in Tab. 3. Notable is linear patterning (Fig. 3A), additionally, oblique or longitudinal cross section of the Haversian canals is visible in relation to FS orientation to the whole bone. Micro-fractures display mainly smooth edges, and respect lamellar arrangement (Fig. 4A). The only exception observed are the micro-cracks lining plate-like protrusions (Fig. 4B), which respect the lamellarity of bone, however their course is in many cases perpendicular to the longitudinal patterning of FS. In helical FS fan-shaped pattern formed by arcuate ridges was observed, crossing the microstructurally conditioned linear pattern (Fig. 3B). This
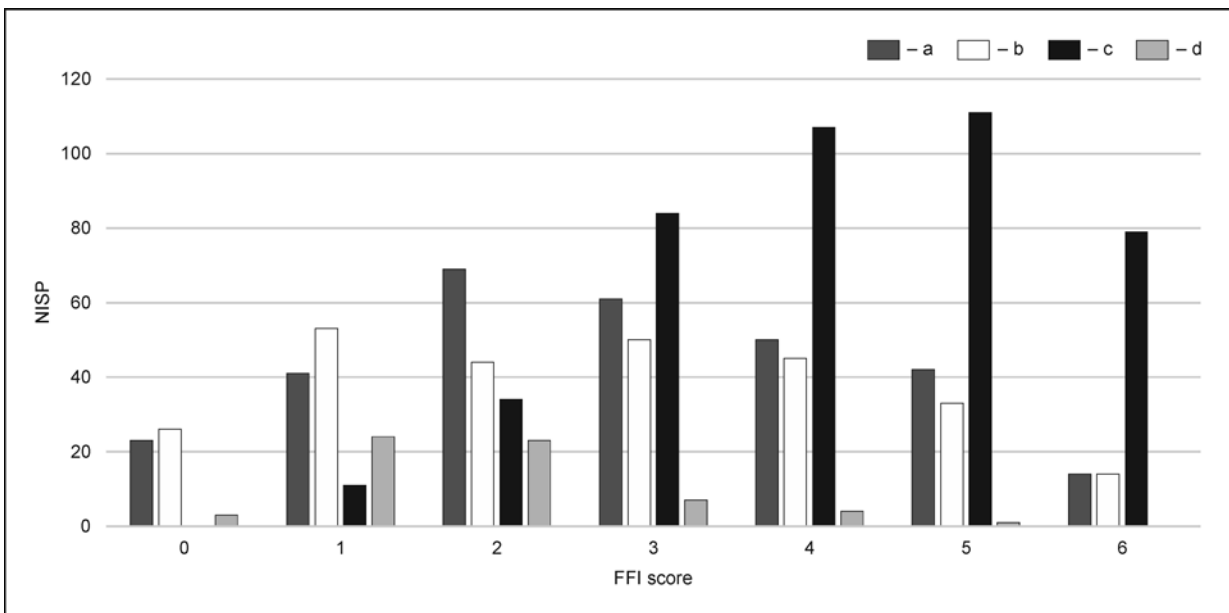
Fig. 2. Representation of individual FFI values in distinct states of preservations and experimental sets. Characteristic distribution according to state of preservation can be observed. Author S. Boriová. Legend: a – fresh bones Set 1; b – frozen bones Set 1; c – dried bones Set 1; d – fresh bones Set 2.

pattern represents the most prominent difference between longitudinal and helical FS. In longitudinal FS individual granular areas were described, also the micro-cracking was generally more pronounced in this type of FS. Histological thin sections showed high uniformity in observed samples, only the surface irregularities were more abundant in longitudinal FS (Tab. 3).

Bones fragmented in frozen state reached the average FFI of 2.75. The distribution of individual FFI scores is very like the fresh samples, with exception of FFI 1 which is significantly higher represented in frozen bones (Fig. 1). Also surface characteristics showed very similar traces to bones fragmented in fresh state (Tab. 3). In one of the longitudinal FS samples, pattern similar to the fan-shaped, but much less pronounced with more diagonal then arcuate trajectory was observed. Occasionally, areas with granular character or plate-like laminar fragmenting were present. One additional type of micro-cracking was observed, typical by irregular reticulate design (Fig. 4C). Observation at the histological level revealed higher variability between longitudinal and helical FS as it was documented in fresh samples. Most distinct was surface morphology (as pictured for example in Fig. 5), small discrepancies were observed also in the location of micro-cracking (Fig. 6A, B; Tab. 3). In some cases, the deflection of fracture by osteon
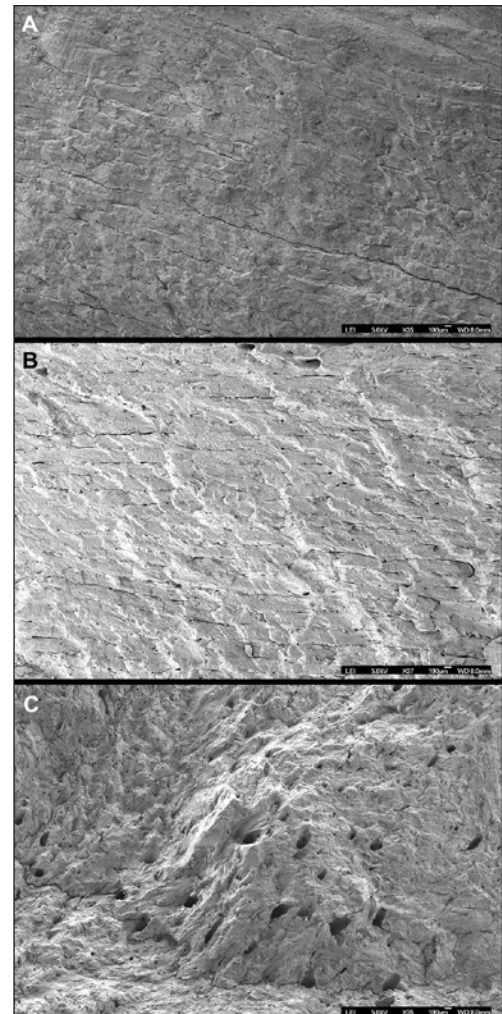

Fig. 3. Examples of observed surface patterns. A – longitudinal FS with linear pattern from fresh bone (sample L, magnification 35×); B – helical FS with fan-shaped pattern from frozen bone (sample E, magnification 37×); C – transversal FS with irregular surface from dried bone (sample J, magnification 35×). Scale bar 100 μm. Photo Z. Pokorná and S. Boriová.

Tab. 3. Summary of main traits observed by the electron and light microscopy. Author S. Boriová.

| | Set1 fresh bones (avg. FFI 2.85) | | Set1 frozen bones (avg. FFI 2.75) | | Set1 dried bones (avg. FFI 4.15) | | Set2 fresh bones with periosteum (avg. FFI 1.9) | |
	longitudinal FS	helical FS	longitudinal FS	helical FS	longitudinal FS	transversal FS	longitudinal FS	helical FS
Surface (SEM)	smooth	smooth	smooth	smooth	rough; granular areas	rough; granular areas	smooth; granular areas	smooth; granular areas
Patterning (SEM)	linear, respecting microstructure	fan-shaped, crossing the linear pattern	linear, respecting microstructure	fan-shaped, crossing the linear pattern	linear, individual ridges rough and bumpy	irregular, not respecting microstructure	fan-shaped pattern less pronounced, linear pattern more apparent	fan-shaped pattern more pronounced, linear pattern less apparent
Micro-cracks (SEM)	longitudinal, respecting the bone microstructure	longitudinal, respecting the bone microstructure	reticular; longitudinal, respecting the bone microstructure	reticular; longitudinal, respecting the bone microstructure	mostly longitudinal course; lining surface irregularities	various course, lining surface irregularities	longitudinal, respecting the bone microstructure	longitudinal, respecting the bone microstructure
Surface profile (HTS)	uniform; smooth	uniform; smooth	mainly uniform; smooth	ambivalent	shaped; variable	shaped; variable	uniform; significantly smooth	uniform; smooth
Surface irregularities (HTS)	mild	isolated	isolated	stepped pattern	stepped pattern	mild	isolated; minimal	isolated; minimal
Micro-fractures (HTS)	short and thin diagonal and perpendicular	short and thin diagonal and perpendicular	short and thin diagonal and perpendicular	short and thin; diagonal emerging in surface depressions	short and thin; diagonal emerging in surface depressions	variable, diagonal and perpendicular; emerging in surface depressions	short and thin diagonal and perpendicular	short and thin diagonal and perpendicular

was observed. Nevertheless, one of the samples (sample M) did not show any of the previously described detailed features.

In dried bones the average FFI reached value of 4.15. In comparison to fresh and frozen bone samples significant shift in surface morphology is observed in both, longitudinal and transversal fracture surfaces. The FSs were generally irregular and rough (Fig. 3C), in certain areas of FS granular character and laminar plate-like cracking was observed. The protrusions and depressions of surface were not respecting the bone microstructure and in most cases were lined by the micro-cracking. In general, the form of micro-cracking was highly variable from wide and long cracks penetrating deep into the sample, to thin and short cracking forming irregular patterns. Significant variability was observed in surface patterning and micro-cracking observed by SEM between longitudinal and transversal FS (Tab. 3). The histological thin sections showed markedly shaped and irregular surface, more pronounced in longitudinal samples (Fig. 5C). Stepped patterning respecting the bone microstructure or various depressions, elevations and protrusions were also places where most of the cracking emerged (Fig. 6C). These cracks show highly variable morphology (Fig. 6D; Tab. 3).

Experimental Set 2

In second experimental set, bones fragmented with periosteum present reached average FFI 1.9. Representation of individual FFI scores in this experimental set can be found in Fig. 1. In comparison to fresh samples from Set 1, the FFI score 1 and 2 were almost evenly represented. Observation of samples under SEM showed morphology consistent with fresh and frozen samples from rockfall experiment. The linear patterning was mostly present at periosteal side of samples and more abundant in longitudinal FS. The most evident difference was given by distinct character of fan-shaped pattern present in both longitudinal and helical FSs. Granular areas were finer in longitudinal FS, whereas in helical ones they were identifiable already in lower overview magnification. Plate-like laminar protrusions were identified again in both types of samples. Micro-cracking was compliant with fresh samples from rockfall experiment. The histological examination revealed uniform and smooth surface profile (Fig. 5A), the smoothness was more pronounced in longitudinal samples. Micro-cracking penetrating the surface was identical to the one observed in rockfall fresh samples, and uniform between longitudinal and helical FSs (Fig. 6A−C).

The summary of the described microscopic features can be found in Tab. 3, the main morphological differences observed in HTSs are pictured in Fig. 5 and 6.

Pavlov I archaeological assemblage

The FFI showed significant differences between the two observed animal species. In the group of wolves, the average FFI score was 4 in area A, 5.5 in area G and 5.2 in area SE014. The most prevalent score for all units is 6, representing fragmentation of bones in a dry state (Fig. 7). The reindeer displayed the average FFI 3.9 for area A, 3 for area G, and 3.8 for area SE014. The most abundant score 3 was documented for all units, meaning fragmentation in less altered state of bone preservation (Fig. 8). A slight deviation can be observed in area SE014 if compared to areas A and G, where a higher number of fragments with low score (2) was observed in wolf material. A score change was observed in reindeer material too, when increased on the upper part of the scoring range (4 if compared to A and G; 6 if compared to G). In order to closely describe the variations in this pattern, the relationship between FFI and spatial distribution of animal bones was examined. Distribution of the two animal species shows certain differences. In case of wolf, the fragmented bones seem to be dispersed more evenly in the studied area, while the fragmented bones of reindeer have tendency to accumulate around the hearth within the unit S1, area SE014 (Fig. 9). No relation between specific FFI values and spatial pattern was observed.

DISCUSSION

Observations from experiments

In our study, the FFI evaluation of experimental assemblages showed several regularities. Not only does the mean value of the index, but also the distribution of values are typical for the three states of preservation. In frozen and fresh bones, the mean value is virtually the same, while the representation of specific values varies a little (Fig. 2). The lower score in frozen samples was observed also by other authors in case of samples frozen for shorter period (one
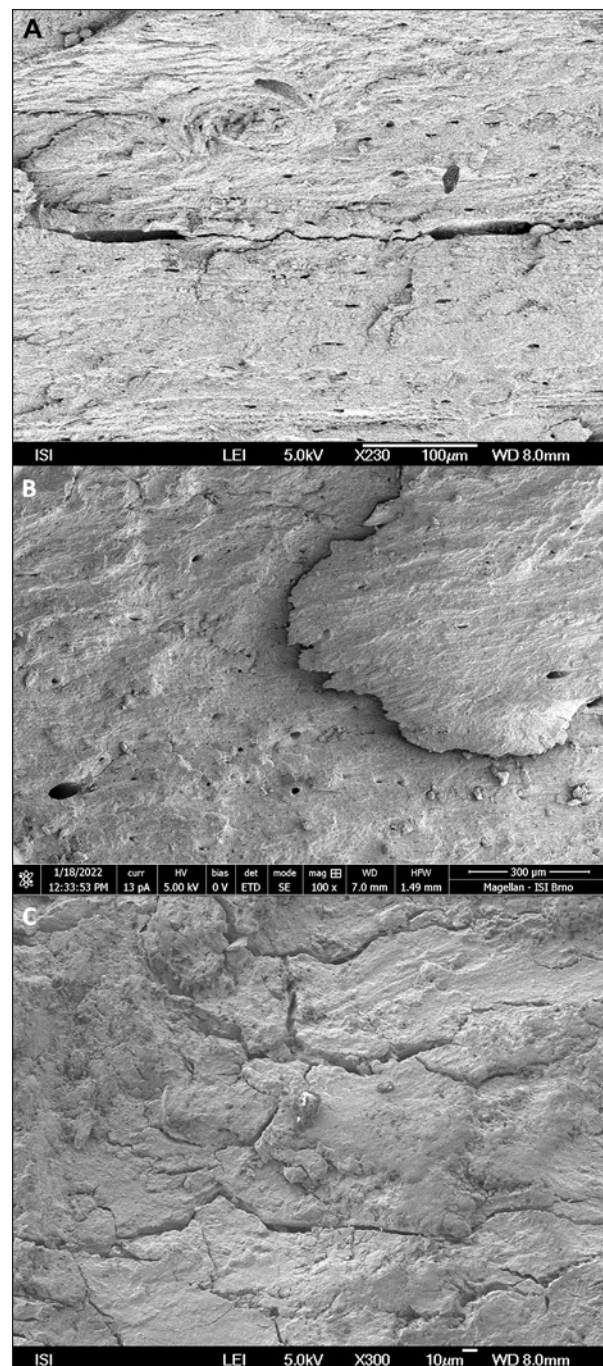

Fig. 4. Types of micro-cracking mostly observed by SEM. A – longitudinal cracking connecting two Haversian canals (sample C, magnification 230×); B – micro-crack lining the plate-like- surface protrusion (sample Q, magnification 100×); C – irregular reticulate micro-cracking observed in frozen samples (sample D, magnification 300×). Photo Z. Pokorná and S. Boriová.

week). The increase of score exceeding the score of fresh bones was observed after several weeks (*Karr/Outram 2012b*). The described phenomenon could be explained by the fact that the bones were fragmented while still frozen. Then, the influence of frozen marrow on specific force transmission within the bone needs to be also considered. Some authors state that the thawing process is the "game-
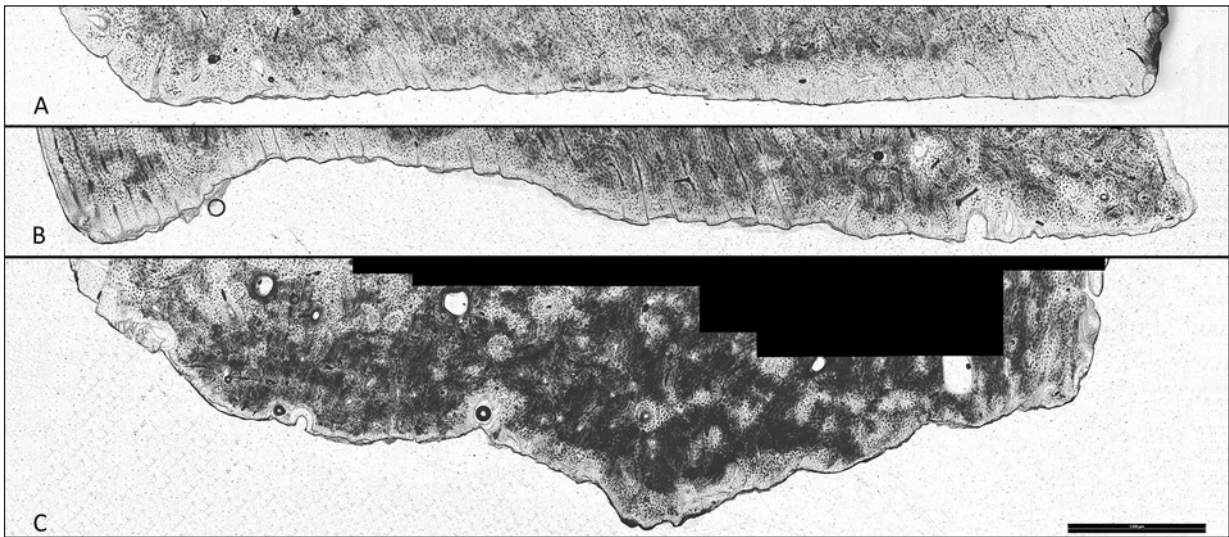
Fig. 5. FS profiles observed on HTS. A – smooth and uniform profile typical for fresh and frozen bones (sample D); B – profile with stepped pattern conditioned by bone structure observed on frozen and dried bones (sample E); C – highly variable and irregular surface profile typical for dried bones (sample G). Magnification 50×, scale bar 1000 μm. Photo S. Boriová.
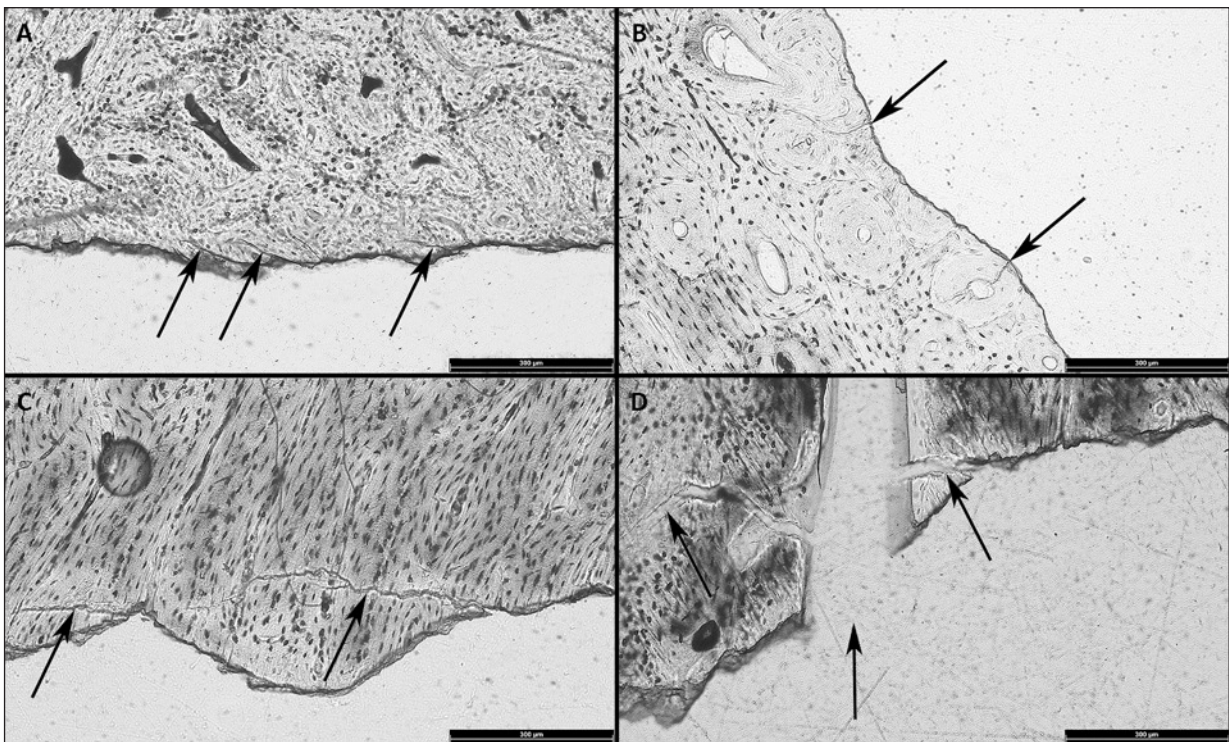

Fig. 6. Different types of micro-fractures observed on HTS indicated by black arrows. A – diagonal (sample Z) and B – perpendicular (sample D) thin and short fractures penetrating the FS; C – diagonal fractures starting in surface depression (sample K); D – variable cracking observed in sample from dried bone (sample J). Magnification 100×, scale bar 300 μm. Photo S. Boriová.

changer" influencing the final fracture morphology and increasing the FFI (*Grunwald 2016*; *Outram 2002*), whereas the degradation following the frozen state takes very slow pace preserving the fresh bone properties. The thawing process results in more significant changes in the bone microstructure providing the characteristic conditions for the fragmentation pattern to change towards the dry state
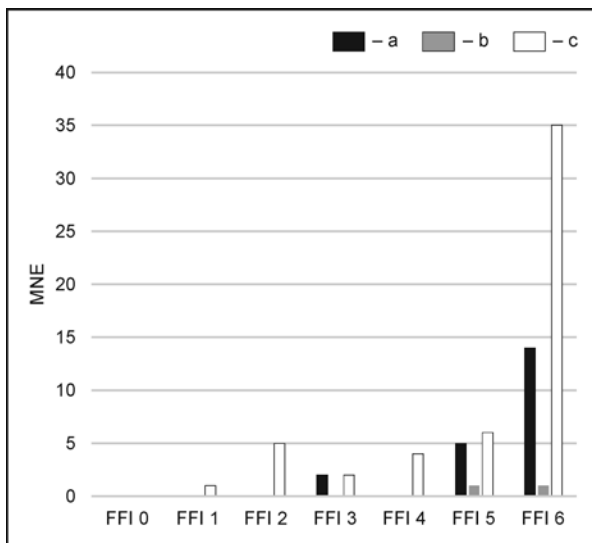
Fig. 7. Pavlov I, area A, G and SE014. Representation of individual FFI scores for fragmented wolf material in selected areas. Author S. Boriová. Legend: a – wolf A; b – wolf G; c – wolf S1.
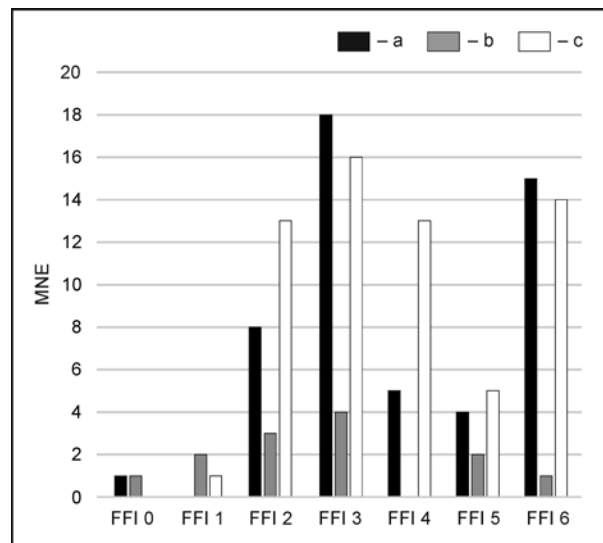
Fig. 8. Pavlov I, area A, G and SE014. Representation of individual FFI scores for fragmented reindeer material in chosen areas. Author S. Boriová. Legend: a – reindeer A; b – reindeer G; c – reindeer S1.

of bone preservation. The dried samples showed significant shift in index value dispersal with an overall value 4 being the most abundant. The rapid moisture loss leads to accelerated bone degradation and alteration of its natural response to applied stress making it highly prone to the transverse failure. Our observations are consistent with results of other experimental works dealing with the state of preservation and using the FFI evaluation system (*Karr 2012*; *Karr/Outram 2012a*; *2012b*; *Outram 2001*; *2002*). Slight difference in mean index values of fresh samples can be observed in the two experimental settings. There are many differences possibly responsible for this variance. Presence of periosteum holds the potential in impacting the number of hits necessary to open the marrow cavity and so frequencies of accompanying BSM (*Blasco et al. 2014*), also in processes of bone alteration it significantly governs the rate of moisture loss and therefore the character of fracture pattern (*Outram 2002*; *Karr/Outram 2012c*). Important variable is also different application of dynamic force. The repeated random nature of impact in rockfall experiment can generate additional micro-cracking, holds potential to introduce wider variety of fragmentation damage, and influence the final FFI score if compared to single hits in controlled marrow extraction. In addition, even different animal species used in both experiments could possibly affect the final index value. The pre-experimental treatment of bones was slightly different too. The fresh bones from the rockfall experiment were refrigerated two weeks prior the experiment, whereas bones fragmented by hammerstone were stored outside in environmental conditions around 9 °C and fragmented in maximum 4 days after the animal was killed. Therefore, further comprehensive experimental work would be desirable to control influence of mentioned variables and test the sensitivity of FFI calculation method.

Observation of samples in SEM similarly revealed morphological differences specific for given states of fractured bones (Tab. 3). Again, quite homogenous traits were identified in fresh and frozen bones. Certain differences were in relation to type of fracture (longitudinal/helical), however, these changes seem to be related mostly to the underlying bone microstructure. The most significant difference observed mainly in fresh samples was fan-shaped pattern of surface, present in helical fractures. It could be related to the specific type of force in combination with given state of bone responsible for bone breakage. Nevertheless, the fan- shaped pattern occurred in both, rockfall and hammerstone broken assemblages. Therefore, we can assume that in studied assemblages this pattern could be specific for dynamic force implementation, however, without being distinctive to the techniques applied. To confirm this hypothesis, it is necessary to examine also other variables which may influence the outcome of the fracturing process. For example, type of precursor (modified/unmodified), type of raw material (hard/soft/inorganic/organic), or application of other than dynamic impact (e.g. *Galán et al. 2009*; *Hutson et al. 2018b*). The micro-fractures in fresh and frozen samples were smooth, and mainly re-
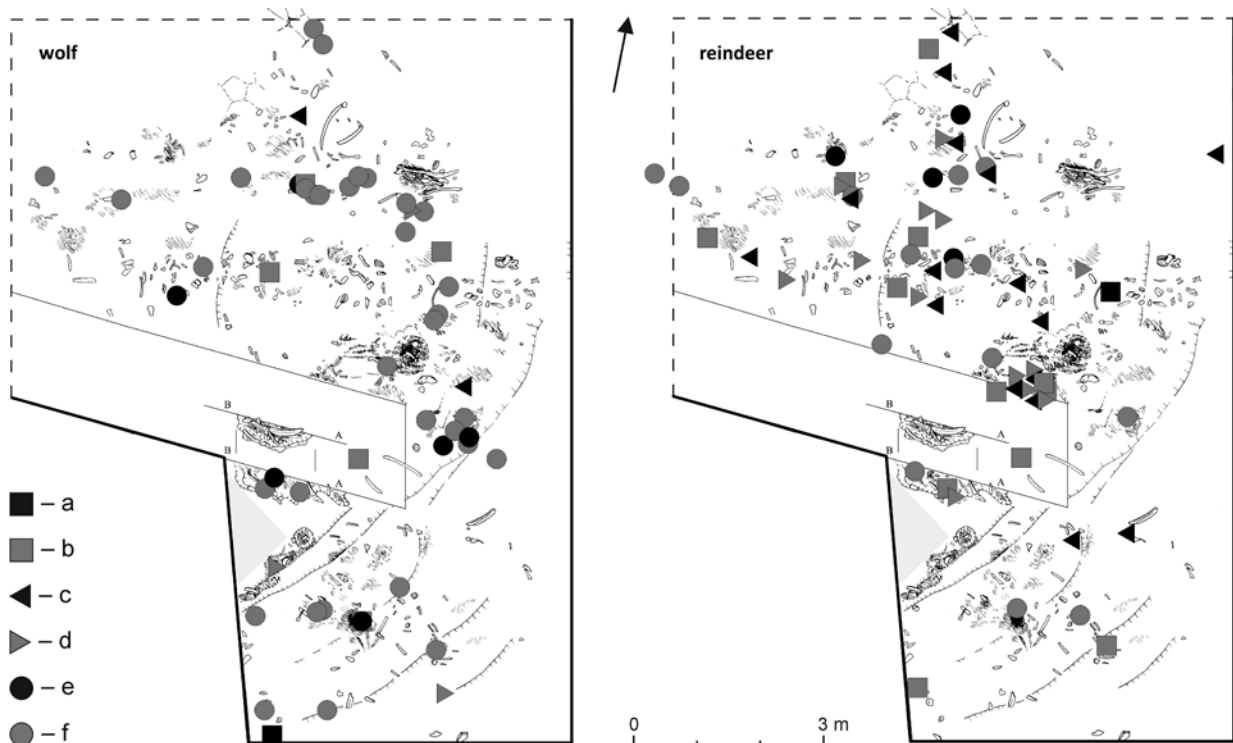
Fig. 9. Pavlov I, area SE014. Spatial distribution of wolf (left area plan) and reindeer (right area plan) fragmented bones according to FFI (according to *Svoboda et al. 2016*, 99, fig. 5). Authors M. Novák and S. Boriová. Legend: a – FFI 1; b – FFI 2; c – FFI 3; d – FFI 4; e – FFI 5; f – FFI 6.

spected the liner and lamellar bone structure. Dried samples again represented separate category with typically irregular rough surface with granular areas. Though, the granular areas were observed also in fresh samples from hammerstone broken assemblage and likely could reflect some of the differences in post-experimental treatment. We were able to identify differences for various kinds of preservation, however clear reference to types stated by *P. Shipman* (*1981*) was not accomplished. This may be due to action of strong dynamic impact in both, rockfall and hammerstone broken assemblages, which according to *P. Shipman* (*1981*) leads to spiral fracture type I. It is typical by propagation of fracture front between the collagen bundles forming smooth surface we described in both fresh and frozen samples from both experimental settings. Nevertheless, it is necessary to bear in mind, that also size of the animal/bone plays an important role in final surface morphology. The smaller is the animal, the relatively greater the force the dynamic effector (falling rock, or hammerstone manipulated by human) can impart to the fractured element, and the higher the probability it exceeds the plasticity in bone response resulting in rough and transverse fractures, even in fresh bones (*Blasco et al. 2014*; *Gifford-Gonzales 2018*). Even though the observed differences are not very pronounced, their presence should stimulate further experimental activities and testing. Analysis of larger sample sets could provide solid background for statistical evaluation of described trace frequencies in relation to anatomical element, bone preservation, acting force, etc. With larger samples sets also methods using machine learning algorithms or artificial intelligence come to mind. In last years they are being successfully applied in BSMs recognition and classification with high accuracy (e.g. *Domínguez-Rodrigo et al. 2020*; *Moclán/Domínguez-Rodrigo/Yravedra 2019*; *Pizarro-Monzo et al. 2022*). These methods hold the potential to similarly address the topic presented in our study. Furthermore, thorough documentation and consistency in pre- and post-experimental treatment should be followed to eliminate other potential sources of surface damage especially when focusing on microscopic surface features (*Karr/Outram 2015*). This way more reliable relation of discovered patterns and differences to the fragmentation process, force or technique implied can be established.

Analysis of histological thin sections revealed presence of three main types of micro-cracking penetrating under the surface. First are cracks associated with the surface irregularities, mostly diagonal in their course (Fig. 6A). Second are fractures perpendicular to fracture surface, mostly respecting the bone

microstructure, very thin and short (Fig. 6B). The third type originates in places of surface irregularities, i.e., depressions, surface protrusions, places of fracture front deflection (Fig. 6C). Unfortunately, no systematic pattern in their presence or frequency was described among the samples subjected to detailed analysis. As more informative seem the fracture surface profile itself. Here we were able to observe the behaviour of fracture front distinctively for different types of preservation (Fig. 5). Deflection of fracture by the main structural units was observed in several cases. Mostly when the fracture front reached the cement line or Haversian canal in transversal cross-section and in some cases when reaching the concentric lamellae in osteons (*O´Brien et al. 2005; Tang et al. 2015*). However, in many cases, without relation to bone preservation the fracture cut right through the osteons without any significant change of course. Only minimal differences for longitudinal and helical fractures were present in HTSs examination. Yet, they may be given rather by the fracture surface orientation and underlying micro-structure than specific type of force or technique responsible for fragmentation.

Relevance for archaeology

Use and function of FFI in archaeological assemblages was already demonstrated by multiple authors (*Karr 2012; Li 2018; Outram 2002*). In order to address issues related to animal body treatment at Moravian Upper Paleolithic sites, we decided to test the usefulness of the index calculation at Pavlov I site. The FFI calculation showed ability to distinguish different fragmentation patterns in different areas within the site. Significant variation was recorded indicating species-dependent manipulation with animal bodies (wolf/reindeer). While wolf long bones showed high FFI scores indicating fracture in a dry state, most probably by different post-depositional processes, reindeer long bones scored lower FFI (average around 3–4) and were most probably a mix of bones fragmented in fresh state for the purpose of marrow exploitation, with additional, later post-depositional fragmentation. This method proved to be able to show not only contrasting treatment of different animal species but also reflect the differences amongst the specific areas within the site (Fig. 7; 8). There is significant difference in representation of lower FFI scores between activity areas (A and G) and settlement area SE014 which is considered to have more overlapping stages/layers (palimpsest) and so may reflect different occupation periods with various ways of animal body treatment. In combination with spatial distribution the detailed fragmentation analysis offers more precise location of presumed processing areas. In case of reindeer, we observed certain accumulative tendency near the hearth, within the settlement area SE014 (Fig. 9). However, when we look at the distribution in relation to FFI no significant accumulations of bones with low index value are visible, they are more or less dispersed evenly in the area of interest. Distinctive cumulative patterns for wolf and reindeer bones are reported also by other researchers for certain accumulations from 1954 and 1956 excavation areas at Pavlov I site (*Musil 2005*). On contrary, in areas excavated in 1952 and 1953 the distribution of reindeer and wolf bones within this site is described as virtually the same but distinct from other, smaller, hunted species. Closer analysis of fracture patterns, as shown in this paper, could provide more detailed information about the state of bone when fragmented and possibly type of force in action. This way, better understanding of the circumstances, agents and purpose of fragmentation process could be achieved. However, to confirm the modest assumptions resulting from microscopic analysis more systematic research needs to be done. Furthermore, applicability of these methods is to great extent influenced by fracture surface preservation. As it was indicated already on the experimental material, the post-fragmentation treatment of bones may play key role in ability to follow described traces. Control for surface preservation state in archaeological specimens would be crucial for final effectiveness of this method.

CONCLUSION

The analytical protocol using two chosen microscopy techniques showed certain ability to reflect distinctive patterns for different states of long bone preservation. The correlation of typical surface changes with mean FFI values in specific samples shows that the changes are most probably related to the state of bone alteration during the fragmentation. The role of specific fragmenting force, skeletal element or animal species in the final form, frequency and representativeness of features needs to be tested to increase the informative value of the studied traces. The analysed features hold a potential in

better understanding and interpretation of archaeological situations related to animal body exploitation, however suitability of these methods according to the state of bone preservation (surface corrosion, cracking and brittleness caused by weathering) must be carefully addressed.

BIBLIOGRAPHY

Alcántara-García et al. 2006
V. Alcántara-García/R. Barba Egido/J. M. Barral del Pino/A. B. Ruiz/A. I. Eiriz Vidal/ Á. Falquina Aparicio/S. Herrero Calleja/A. Ibarra Jiménez/M. Megías González/ M. Pérez Gil/V. Pérez Tello/J. Rolland Calvo/J. Yravedra Sáinz de los Terreros/A. Vidal/ M. Domínguez-Rodrigo: Determinación de procesos de fractura sobre huesos: un sistema de análisis de los ángulos de los planos de fracturación como discriminador de agentes bióticos. *Trabajos de Prehistoria* 61, 2006, 25–38.

Binford 1981
L. R. Binford: *Bones: ancient man and modern myths.* San Diego 1981.

Blasco et al. 2014
R. Blasco/M. Domínguez-Rodrigo/M. Arilla/E. Camarós/J. Rosell: Breaking Bones to Obtain Marrow. A Comparative Study Between Percussion by Batting Bone on an Anvil and Hammerstone Percussion. *Archaeometry* 56, 2014, 1085–1104.
DOI: https://doi.org/10.1111/arcm.12084

Blumenschine 1995
R. J. Blumenschine: Percussion marks, tooth marks and experimental determinations of the timing of hominid and carnivore access to long bones at FLK Zinjanthropus. *Journal of Human Evolution* 29, 1995, 21–51.
DOI: https://doi.org/10.1006/jhev.1995.1046

Bonnichsen 1979
R. Bonnichsen: *Pleistocene bone technology in the Beringian Refugium.* Ottawa 1979.

Bradfield/Brand 2015
J. Bradfield/T. Brand: Results of utilitarian and accidental breakage experiments on bone points. *Archaeological and Anthropological Sciences* 7, 2015, 27–38.
DOI: https://doi.org/10.1007/s12520-013-0136-5

Capaldo 1997
S. D. Capaldo: Experimental determination of carcass processing by Plio-Pleistocene hominids and carnivores at FLK 22 (Zinjanthropus). *Journal of Human Evolution* 33, 1997, 555–597.
DOI: https://doi.org/10.1006/jhev.1997.0150

Capaldo/Blumenschine 1994
S. D. Capaldo/R. J. Blumenschine: A quantitative diagnosis of notches made by hammerstone percussion and carnivore gnawing in bovid long bones. *American Antiquity* 59, 1994, 724–748.
DOI: https://doi.org/10.2307/282345

Coil/Tappen/Yezzi-Woodley 2017
R. Coil/M. Tappen/K. Yezzi-Woodley: New Analytical Methods for Comparing Bone Fracture Angles. A Controlled Study of Hammerstone and Hyena (Crocuta crocuta) Long Bone Breakage. *Archaeometry* 59, 2017, 900–917.
DOI: https://doi.org/10.1111/arcm.12285

Currey 2002
J. D. Currey: *Bones: structures and mechanics.* Oxford 2002.

Currey 2012
J. D. Currey: The structure and mechanics of bone. *Journal of Material Sciences* 47, 2012, 41–54.
DOI: https://doi.org/10.1007/s10853-011-5914-9

Domínguez-Rodrigo 2002
M. Domínguez-Rodrigo: Hunting and Scavenging by Early Humans: The State of the Debate. *Journal of World Prehistory* 16, 2002, 1–54.
DOI: https://doi.org/10.1023/A:1014507129795

Domínguez-Rodrigo/Barba 2006
M. Domínguez-Rodrigo/R. Barba: New estimates of tooth mark and percussion mark frequencies at the FLK Zinj site: the carnivore-hominid-carnivore hypothesis falsified. *Journal of Human Evolution* 50, 2006, 170–194.
DOI: https://doi.org/10.1016/j.jhevol.2005.09.005

Domínguez-Rodrigo et al. 2020
M. Domínguez-Rodrigo/G. Cifuentes-Alcobendas/B. Jiménez-García/N. Abellán/ M. Pizarro-Monzo/E. Organista/E. Baquedano: Artifcial intelligence provides greater accuracy in the classifcation of modern and ancient bone surface modifications. *Nature Scientific Reports* 10, 2020, 18862.
DOI: https://doi.org/10.1038/s41598-020-75994-7

Evans 1957
F. G. Evans: *Stress and strain in bones. Their relation to fractures and osteogenesis.* Springfield 1957.

Galán et al. 2009
A. B. Galán/M. Rodríguez/S. de Juana/M. Domínguez-Rodrigo: A new experimental study on percussion marks and notches and their bearing on the interpretation of

	hammerstone-broken faunal assemblages. *Journal of Archaeological Science* 36, 2009, 776–784. DOI: https://doi.org/10.1016/j.jas.2008.11.003
Gifford-Gonzales 2018	D. Gifford-Gonzales: *An Introduction to Zooarchaeology*. Santa Cruz 2018. DOI: https://doi.org/10.1007/978-3-319-65682-3
Grunwald 2016	A. M. Grunwald: Analysis of fracture patterns from experimentally marrow-cracked frozen and thawed cattle bones. *Journal of Archaeological Science* 8, 2016, 356–365. DOI: https://doi.org/10.1016/j.jasrep.2016.06.022
Haglund/Sorg 2002	W. D. Haglund/M. H. Sorg: Human remains in water environments. In: W. G. Haglund/M. H. Sorg (eds.): *Advances in forensic taphonomy: method, theory and archaeological perspectives*. Florida 2002, 201–218. DOI: https://doi.org/10.1201/9781420058352
Hamed/Lee/Jasiuk 2010	E. Hamed/Y. Lee/I. Jasiuk: Multiscale modelling of elastic properties of cortical bone. *Acta Mechanica* 213, 2010, 131–154. DOI: https://doi.org/10.1007/s00707-010-0326-5
Haynes 1983	G. Haynes: Frequencies of spiral and green-bone fractures on ungulate limb bones in modern surface assemblages. *American Antiquity* 48, 1983, 102–114. DOI: https://doi.org/10.2307/279822
Haynes/Krasinski/Wojtal 2021	G. Haynes/K. Krasinski/P. Wojtal: Study of Fractured Proboscidean Bones in Recent and Fossil Assemblages. *Journal of Archaeological Method and Theory* 28, 2021, 956–1025. DOI: https://doi.org/10.1007/s10816-020-09486-3
Hedges/Millard 1995	R. E. M. Hedges/A. R. Millard: Bones and Groundwater: Towards the Modelling of Diagenetic Processes. *Journal of Archaeological Science* 22, 1995, 155–164. DOI: https://doi.org/10.1006/jasc.1995.0017
Hutson et al. 2018a	J. M. Hutson/A. García-Moreno/E. S. Noack/E. Turner/A. Villaluenga/S. Gaudzinski-Windheuser: *The Origins of Bone Tool Technologies*. Mainz 2018. DOI: https://doi.org/10.11588/propylaeum.408
Hutson et al. 2018b	J. M. Hutson/A. Villaluenga/A. García-Moreno/E. Turner/S. Gaudzinski-Windheuser: On the use of metapodials hammers as tools at Schöningen 13II-4. In: *Hutson et al. 2018a*, 53–91. DOI: https://doi.org/10.11588/propylaeum.408
Johnson 1985	E. Johnson: Current Developments in Bone Technology. *Advances in Archaeological Method and Theory* 8, 1985, 157–235. DOI: https://doi.org/10.1016/B978-0-12-003108-5.50010-5
Johnson/Parmenter/Outram 2016	E. V. Johnson/P. C. R. Parmenter/A. K. Outam: A new approach to profiling taphonomic history through bone fracture analysis, with an example application to the Linearbandkeramik site of Ludwinowo 7. *Journal of Archaeological Science* 9, 2016, 623–629. DOI: https://doi.org/10.1016/j.jasrep.2016.08.047
Karr 2012	L. P. Karr: *The Analysis and Interpretation of Fragmented Mammoth Bone Assemblages: Experiments in Bone Fracture with Archaeological Applications*. Dissertation thesis. University of Exeter. Exeter 2012. Unpublished.
Karr/Outram 2012a	L. P. Karr/ A. K. Outram A.K.: Bone Degradation and Environment: Understanding, Assessing and Conducting Archaeological Experiments Using Modern Animal Bones. *International Journal of Osteoarchaeology* 25, 2012, 201–212. DOI: https://doi.org/10.1002/oa.2275
Karr/Outram 2012b	L. P. Karr/ A. K. Outram: Tracking changes in bone fracture morphology over time: environment, taphonomy, and the archaeological record. *Journal of Archaeological Science* 39, 2012, 555–559. DOI: https://doi.org/10.1016/j.jas.2011.10.016
Karr/Outram 2012c	L. P. Karr/A. K. Outram: Actualistic research into dynamic impact and its implications for understanding differential bone fragmentation and survivorship. *Journal of Archaeological Science* 39, 2012, 3443–3449. DOI: https://doi.org/10.1016/j.jas.2012.05.013
Karr/Outram 2015	L. P. Karr/A. K. Outram: Bone Degradation and Environment: Understanding, Assessing and Conducting Archaeological Experiments Using Modern Animal Bones. *International Journal of Osteoarchaeology* 25 (2), 2015, 201–212. DOI: https://doi.org/10.1002/oa.2275
Li/Abdel-Wahab/Silberschmidt 2013	S. Li/A. Abdel-Wahab/V. V. Silberschmidt: Analysis of fracture processes in cortical bone tissue. *Engineering Fracture Mechanics* 110, 2013, 448–458. DOI: https://doi.org/10.1016/j.engfracmech.2012.11.020
Li 2018	X. Li: *What did the fox say? Assessing the role of foxes through ethnographic and archaeological contexts*. Dissertation thesis. University of Exeter. Exeter 2018. Unpublished.
Lyman 1994	R. L. Lyman: *Vertebrate taphonomy*. Cambridge 1994.
Marean et al. 2000	C. W. Marean/Y. Abe/C. J. Frey/R. C. Randall: Zooarchaeological and taphonomic analysis of the Die Kelders Cave 1 Layers 10 and 11 Middle Stone Age larger mammal fauna.

Journal of Human Evolution 38, 2000, 197–233.
DOI: https://doi.org/10.1006/jhev.1999.0356

Merritt/Davis 2017 — S. R. Merritt/K. M. Davis: Diagnostic properties of hammerstone-broken long bone fragments, specimen identifiability and Early Stone Age butchered assemblage interpretation. *Journal of Archaeological Science* 85, 2017, 114–123.
DOI: https://doi.org/10.1016/j.jas.2017.06.009

Moclán/Domínguez-Rodrigo/Yravedra 2019
A. Moclán/M. Domínguez-Rodrigo/J. Yravedra: Classifying agency in bone breakage: an experimental analysis of fracture planes to differentiate between hominin and carnivore dynamic and static loading using machine learning (ML) algorithms. *Archaeological and Anthropological Sciences* 11, 2019, 4663–4680.
DOI: https://doi.org/10.1007/s12520-019-00815-6

Morlan 1984 — R. Morlan: Toward the Definition of Criteria for the Recognition of Artificial Bone Alterations. *Quaternary Research* 22, 1984, 160–171.
DOI: https://doi.org/10.1016/0033-5894(84)90037-1

Musil 2005 — R. Musil: Animal Prey. In: *Pavlov I Southeast. A window Into the Gravettian Lifestyle.* Academy of Sciences of the Czech Republic. Brno 2005, 190–228.

O´Brien et al. 2005 — F. J. O´Brien/D. A. Hardiman/J. G. Hazenberg/ M. V. Mercy/S. Mohsin/D. Taylor/ T. C. Lee: The behaviour of microcracks in compact bone. *European Journal of Morphology* 42, 2005, 71–79.
http://dx.doi.org/10.1080/ejom.42.1-2.0071

Organista et al. 2016 — E. Organista/M. Pernas-Hernández/A. Gidna/J. Yravedra/M. Domínguez-Rodrigo: An experimental lion-to-hammerstone model and its relevance to understand hominin-carnivore interactions in the archeological record. *Journal of Archaeological Science* 66, 2016, 69–77.
DOI: https://doi.org/10.1016/j.jas.2015.12.004

Outram 2001 — A. K. Outram: A New Approach to Identifying Bone Marrow and Grease Exploitation: Why the "Indeterminate" Fragments Should Not be Ignored. *Journal of Archaeological Science* 28, 2001, 401–410.
DOI: https://doi.org/10.1006/jasc.2000.0619

Outram 2002 — A. K. Outram: Bone fracture and within-bone nutrients: An experimentally based method for investigating levels of marrow extraction. In: P. Miracle/N. Milner (eds.): *Consuming Passions and Patterns of Consumption.* Cambridge 2002, 51–64.

Parkinson 2018 — J. Parkinson: Revisiting the hunting-versus-scavenging debate at FLK Zinj: A GIS spatial analysis of bone surface modifications produced by hominins and carnivores in the FLK 22 assemblage. *Palaeogeography, Palaeoclimatology, Palaeoecology* 511, 2018, 29–51.
DOI: https://doi.org/10.1016/j.palaeo.2018.06.044

Pizarro-Monzo et al. 2022 — M. Pizarro-Monzo/E. Organista/L. Cobo-Sánchez/E. Bequedano/M. Domínguez-Rodrigo: Determining the diagenetic paths of archaeofaunal assemblages and their palaeoecology through artificial intelligence: an application to Oldowan sites from Olduvai Gorge (Tanzania). *Journal of Quaternary Science* 37 (3), 2022, 543–557.
DOI: https://doi.org/10.1002/jqs.3385

Pickering/Egeland 2006 — T. R. Pickering/C. P. Egeland: Experimental patterns of hammerstone percussion damage on bones and zooarchaeological inferences of carcass processing intensity by humans. *Journal of Archaeological Science* 33, 2006, 459–469.
DOI: https://doi.org/10.1016/j.jas.2005.09.001

Rho/Kuhn-Spearing/Zioupos 1998 — J. Y. Rho/L. Kuhn-Spearing/P. Zioupos: Mechanical properties and the hierarchical structure of bone. *Medical Engineering and Physics* 20, 1998, 92–102.
DOI: https://doi.org/10.1016/S1350-4533(98)00007-1

Sázelová/Boriová/Šáliová 2021 — S. Sázelová/S. Boriová/S. Šáliová: The Upper Paleolithic hard animal tissue under the microscope: Selected examples from Moravian sites. *Quaternary International* 587–588, 2021, 127–136.
DOI: https://doi.org/10.1016/j.quaint.2020.10.027

Shipman 1981 — P. Shipman: Applications of scanning electron microscopy to taphonomic problems. In: A.-M. E. Cantwell/J. B. Griffin/N. A. Rothschild (eds.): *The research potential of anthropological museum collections.* New York 1981, 357–386.

Stanford/Bonnichsen/Morlan 1981 — D. Stanford/R. Bonnichsen/R. E. Morlan: The Ginsberg experiment. Modern and prehistoric evidence of a bone-flaking technology. *Science* 212, 1981, 438–440.
DOI: https://doi.org/10.1126/science.212.4493.438

Stiner 2004 — M. C. Stiner: Comparative ecology and taphonomy of spotted hyenas, humans and wolves in Pleistocene Italy. *Revue de Paléobiologie* 23, 2004, 771–785.

Svoboda et al. 2016 — J. Svoboda/M. Novák/S. Sázelová/J. Demek: Pavlov I. A large Gravettian site in space and time. *Quaternary International* 406, 2016, 95–105.
DOI: https://doi.org/10.1016/j.quaint.2015.09.015

Tang et al. 2015	T. Tang/V. Ebacher/P. Cripton/P. Guy/H. McKay/R. Wang: Shear deformation and fracture of human cortical bone. *Bone* 71, 2015, 25–35. DOI: https://doi.org/10.1016/j.bone.2014.10.001
Tappen 1969	N. C. Tappen: The relationship of weathering cracks to split-line orientation in bone. *American Journal of Physical Anthropology* 31, 1969, 191–197.
Tappen/Peske 1970	N. C. Tappen/ R. Peske: Weathering Cracks and Split-Line Patterns in Archaeological Bone. *Antiquity* 35, 1970, 383–386. DOI: https://doi.org/10.2307/278350
Thompson et al. 2017	J. C. Thompson/ J. T. Faith/ N. Cleghorn/ J. Hodgkins: Identifying the accumulator: Making the most of bone surface modification data. *Journal of Archaeological Science* 85, 2017, 105–113. DOI: https://doi.org/10.1016/j.jas.2017.06.013
Thompson et al. 2019	J. C. Thompson/S. Carvalho/C. W. Marean/Z. Alemseged: Origins of the Human Predatory Pattern. The Transition to Large-Animal Exploitation by Early Hominins. *Current Anthropology* 60, 2019, 1–23. DOI: https://doi.org/10.1086/701477
Thorson/Guthrie 1984	R. M. Thorson/R. D. Guthrie: River ice as a taphonomic agent: An alternative hypothesis for bone "artifacts". *Quaternary Research* 22, 1984, 172–188.
Vettese et al. 2020	D. Vettese/R. Blasco/I. Cáceres/S. Gaudzinski-Windheuser/M.-H. Moncel/U. Thun Hohenstein/C. Daujeard: Towards an understanding of hominin marrow extraction strategies: a proposal for a percussion mark terminology. *Archaeological and Anthropological Science* 12 (48), 2020. DOI: https://doi.org/10.1007/s12520-019-00972-8
Vettese et al. 2021	D. Vettese/T. Stavrova/A. Borel/J. Marín/M.-H. Moncel/M. Arzarello/C. Daujeard: A way to break bones? The weight of intuitiveness. *PLoS ONE* 16, 2021, e0259136. DOI: https://doi.org/10.1371/journal.pone.0259136
Villa/Mahieu 1991	P. Villa/E. Mahieu: Breakage patterns of human long bones. *Journal of Human Evolution* 21, 1991, 27–48. DOI: https://doi.org/10.1016/0047-2484(91)90034-S
Wang 2011	X. Wang: Cortical Bone Mechanics and Composition: Effects of Age and Gender. In: M. Silva (eds.): *Skeletal Aging and Osteoporosis. Studies in Mechanobiology*. Tissue Engineering and Biomaterials 5. Heidelberg 2011. DOI: https://doi.org/10.1007/8415_2011_108
Waterhouse 2013	K. Waterhouse: The effect of weather conditions on burnt bone fragmentation. *Journal of Forensic and Legal Medicine* 20, 2013, 489–495. DOI: https://doi.org/10.1016/j.jflm.2013.03.016
Zioupos/Kirchner/Peterlik 2020	P. Zioupos/H. O. K. Kirchner/H. Peterlik: Ageing bone fractures: the case of ductile to brittle transition that shifts with age. *Bone* 131, 2020, 1–11. DOI: https://doi.org/10.1016/j.bone.2019.115176

Lomy na kostiach pod mikroskopom

Experimentálny prístup k analýze zvieracích kostí z mladého paleolitu

Soňa Boriová – Alan K. Outram – Zuzana Pokorná – Sandra Sázelová

Súhrn

Fragmentarizácia kostí na archeologických lokalitách môže byť dôkazom pôsobenia širokej škály prírodných procesov a tafonomických činiteľov. Výnimkou nie je ani človek, ktorý kosti lámal zámerne za účelom získania živín alebo suroviny. Modifikácie, ktoré pri týchto procesoch vznikajú na povrchu kostí môžu byť špecifické pre daného činiteľa, avšak v mnohých prípadoch sa vo svojej forme vzájomne prekrývajú. Výslednú formu fragmentarizačných stôp neovplyvňuje iba druh aktivity/činiteľa. Dôležitú rolu zohráva taktiež celkový tvar a veľkosť kosti, jej mikroskopická stavba či aktuálny stav zachovania. Rozsiahla experimentálna činnosť v oblasti fragmentarizácie cicavčích

dlhých kostí v posledných desaťročiach priniesla popis určitých znakov, ktoré nám takéto rozlíšenie umožňujú. Ide najmä o znaky makroskopické, popisujúce uhol lomu voči povrchu kompaktnej kosti, tvar/priebeh lomu a textúru povrchu lomu, prípadne sprievodné povrchové modifikácie. Takouto metódou je napríklad určovanie fragmentarizačného indexu (FFI, *Outram 2001*), ktorý sme využili aj pri hodnotení skúmaného experimentálneho materiálu. V štúdii sme využili elektrónovú a svetelnú mikroskopiu pre detailné zobrazenie povrchu lomu a preskúmanie vznikajúcich mikroprasklín. Cieľom bolo zistiť, či rozdiely vo fragmentarizácii existujú aj na mikroskopickej úrovni a či je možné mikroskopické znaky korelovať s výsledkami makroskopického pozorovania. Vybrané mikroskopické metódy sme testovali na dvoch experimentálnych súboroch kostí, ktoré vznikli použitím rôzneho druhu dynamickej sily. V prvej zbierke (Set 1) boli fragmentarizované kosti v čerstvom zmrazenom a sušenom stave sériou pádov kameňov. V druhej zbierke (Set 2) išlo o čerstvé kosti so zachovanou okosticou, fragmentarizované pomocou kamenného otĺkača a nákovy. Skúmaných bolo celkom 24 vzoriek (obr. 1). Set 1 bol zastúpený vždy 4 vzorkami pre každý stav zachovania, 2 vzorky pozdĺžneho lomu a 2 špirálovitého lomu, v prípade sušených kostí 2 vzorky transverzálneho lomu. Set 2 je zastúpený 6 vzorkami pozdĺžneho a 6 vzorkami špirálovitého lomu. Pozorovanie pomocou SEM ukázalo niekoľko výraznejších znakov, charakteristických pre typ lomu a zachovanie kosti. V prípade čerstvých a zmrazených vzoriek (Set 1) boli pozorované znaky veľmi podobné, a to hladký povrch lomu s lineárnym vzorom rešpektujúcim mikroštruktúru kosti (obr. 3A). V prípade vzoriek zo špirálovitých lomov sme pozorovali typický vejárovitý vzor (obr. 3B), krížiaci lineárny vzor. Mikropraskliny mali u čerstvých a zmrazených vzoriek veľmi podobný charakter. Nachádzali sa hlavne pozdĺžne v súlade s mikroštruktúrou kosti (obr. 4A), prípadne lemovali povrchové nerovnosti alebo plátovité výbežky (obr. 4B). Výnimkou boli sieťovité praskliny pozorované na pozdĺžnych aj špirálovitých lomoch zmrazených kostí (obr. 4C). Takmer zhodné boli aj priemerné hodnoty fragmentarizačného indexu (FFI) a to 2,85 pre kosti čerstvé a 2,75 pre kosti zmrazené. Výrazne odlišná morfológia povrchu bola pozorovaná na vzorkách zo sušených kostí (Set 1). V prípade pozdĺžnych lomov bolo možné identifikovať lineárny vzor, avšak povrch bol celkovo drsný s granulárnymi oblasťami a v prípade priečnych lomov s veľmi nepravidelným tvarovaním (obr. 3C). Charakter mikroprasklín bol variabilnejší ako v prípade čerstvých a sušených kostí. Najpočetnejšie boli praskliny pozdĺžne alebo lemujúce povrchové nerovnosti. Sušené kosti sa líšili aj nápadne vyššou hodnotou FFI (4,15). Histologické výbrusy ukázali typické odlišnosti týkajúce sa profilu povrchu lomu. U vzoriek čerstvých a zmrazených bol profil väčšinou hladký, jednotný, nevýrazne tvarovaný, s ojedinelými výbežkami/priehlbinami (obr. 5A). V prípade zmrazených kostí sme pozorovali ohnutie roviny šírenia lomu v štrukturálne odlišných častiach, akými sú napríklad cementové línie alebo koncentrické lamely osteónov (obr. 5B). Pri sušených vzorkách bol profil výrazne odlišný od predchádzajúcich dvoch, bol variabilný a tvarovaný (obr. 5C). Pozorovanie na histologických výbrusoch odhalilo hlavné typy mikroprasklín, ktoré prenikali pod povrch lomu. Išlo o krátke a tenké praskliny s diagonálnym (obr. 6A) alebo kolmým (obr. 6B) priebehom a začínajúce praskliny v povrchových priehlbinách, opäť prenikajúcich do vzorky s diagonálnym priebehom (obr. 6C). Najväčšia variabilita bola pozorovaná u vzoriek zo sušených kostí, avšak bližšie charakteristické zastúpenie pre jednotlivé stavy zachovania kosti nebolo pozorované (obr. 6D). Vzorky čerstvých kostí z druhého experimentu (Set 2) vykazovali znaky zhodné s čerstvými kosťami z toho predošlého (Set 1), ako pri pozorovaní na SEM, tak na úrovni histologickej. Výraznejšou odlišnosťou bola len nižšia hodnota FFI (1,90). Predpokladáme, že príčinou môže byť použitie odlišnej techniky dynamickej sily, opakovaný náraz pri páde kameňov, ale potenciálne aj prítomnosť okostice (*periosteum*). Výsledky mikroskopického pozorovania ukázali, že spolu s výraznejšími zmenami v stave zachovania kosti dochádza aj k výraznejším zmenám v mikromorfologických znakoch, akými je vzor povrchu lomu alebo tvar a priebeh mikroprasklín. Tieto výsledky sú zhodné s hodnotením pomocou FFI. V porovnaní s makroskopickou metódou nám štúdium mikroskopických znakov v prezentovanom rozsahu neumožnilo detailnejšie rozlíšenie, napríklad medzi lomami vzniknutými na čerstvých a zmrazených kostiach.

Hodnotenie prostredníctvom FFI sme aplikovali na vybraný materiál z plochy G, A a S1 gravettienskej lokality Pavlov I. Zamerali sme sa na dva zvieracie druhy (vlk, sob), u ktorých predpokladáme odlišnú motiváciu k zámernej exploatácii človekom. Výsledky makroskopického hodnotenia ukázali, že hodnota FFI je zhodná naprieč vybranými plochami a odlišná pre konkrétne druhy. V prípade vlčích kostí bola priemerná hodnota indexu v rozmedzí 4–5,5, čo naznačuje fragmentarizáciu v značne pozmenenom stave (výrazná strata vlhkosti), pravdepodobne najmä postdepozičnými procesmi. V prípade kostí sobov sme zaznamenali priemernú hodnotu indexu v rozmedzí 3–3,9. Tá poukazuje na zmiešaný charakter fragmentarizačnej histórie, teda kombináciu lomov vznikajúcich na čerstvej ale aj suchej kosti. Mierne odlišné zastúpenie jednotlivých skóre bolo pozorované pre oba druhy na ploche S1, a mohlo by tak poukazovať na odlišnú funkciu či vyššiu komplexnosť tejto sídelnej jednotky v porovnaní so plochami A a G (obr. 7; 8). Súvislosť medzi priestorovou distribúciou jednotlivých fragmentov a ich FFI hodnotou sa nepodarilo preukázať (obr. 9). Podrobnejšia analýza stôp fragmentarizácie, ako ukazujeme v príspevku, by mohla poskytnúť detailnejšie informácie o stave zachovania kosti a prípadne aj type sily, ktorá kosť polámala. Získané poznatky by tak mohli prispieť k lepšiemu pochopeniu okolností či účelu fragmentarizácie kosteného materiálu. Pre overenie hypotéz, ktoré vyplynuli z našich mikroskopických pozorovaní je však nutný hlbší systematický výskum. Aplikovateľnosť navrhnutých metód na archeologický materiál je do veľkej miery závislá na stave zachovania povrchu kostí. Preto jeho kontrola pred aplikáciou mikroskopických metód bude hrať kľúčovú rolu pri určovaní finálnej efektívnosti.

Obr. 1. Ukážka vzorkovania na SEM a príprava histologických výbrusov. Špirálovitý lom, vzorka Q, Set 2. Foto S. Boriová.

Obr. 2. Zastúpenie jednotlivých hodnôt FFI v rôznych stavoch zachovania a experimentálnych behoch. Distribúcia je charakteristická pre konkrétny stav zachovania kostí. Autor S. Boriová. Legenda: a – čerstvé kosti Set 1; b – zmrazené kosti Set 1; c – sušené kosti Set 1; d – čerstvé kosti Set 2.

Obr. 3. Ilustračné príklady pozorovaných povrchových vzorov. A – povrch pozdĺžneho povrch lomu s lineárnym vzorom na čerstvej kosti (vzorka L, priblíženie 35×); B – povrch špirálovitého lomu s vejárovitým vzorom na zmrazenej kosti (vzorka E, priblíženie 37×); C – povrch transverzálneho lomu s výrazne nepravidelným povrchom na sušenej kosti (vzorka J, priblíženie 35×). Mierka 100 μm. Foto Z. Pokorná a S. Boriová.

Obr. 4. Najčastejšie pozorované typy mikroprasklín pomocou SEM. A – pozdĺžna prasklina spájajúca dva Haversove kanáliky (vzorka C, priblíženie 230×); B – mikroprasklina lemujúca diskovitý/plátkovitý výbežok (vzorka Q, priblíženie 100×); C – nepravidelné sieťovité mikropraskliny pozorované na vzorkách zo zmrazených kostí (vzorka D, priblíženie 300×). Foto Z. Pokorná a S. Boriová.

Obr. 5. Profily povrchu lomov pozorované na histologických výbrusoch. A – hladký a jednotný profil typický pre čerstvé a zmrznuté kosti (vzorka D); B – profil so schodkovitým priebehom podmienený mikroštruktúrou kosti pozorovaný na zmrznutých aj sušených kostiach (vzorka E); C – výrazne variabilný a nepravidelný profil povrchu typický pre sušené kosti (vzorka G). Priblíženie 50×, mierka 1000 μm. Foto S. Boriová.

Obr. 6. Čierne šípky ukazujú na rôzne typy mikroprasklín pozorované prostredníctvom histologických výbrusov. A – diagonálne (vzorka Z) a B – kolmé (vzorka D) tenké, krátke praskliny idúce pod povrch lomu; C – diagonálne praskliny začínajúce v povrchovej priehlbine (vzorka K); D – rôznorodé praskliny pozorované na vzorke zo sušenej kosti (vzorka J). Priblíženie 100×, mierka 300 μm. Foto S. Boriová.

Obr. 7. Pavlov I, plocha A, G a SE014. Zastúpenie jednotlivých hodnôt FFI pre fragmentarizované kosti vlkov vo vybraných plochách. Autorka S. Boriová. Legenda: a – vlk A; b – vlk G; c – vlk S1.

Obr. 8. Pavlov I, plocha A, G a SE014. Zastúpenie jednotlivých hodnôt FFI pre fragmentarizované kosti sobov vo vybraných plochách. Autorka S. Boriová. Legenda: a – sob A; b – sob G; c – sob S1.

Obr. 9. Pavlov I, plocha SE014. Priestorová distribúcia vlčích (ľavý plán plochy) a sobích (pravý plán plochy) fragmentarizovaných kostí vo vzťahu k hodnote FFI (podľa *Svoboda et al. 2016*, 99, obr. 5). Autori M. Novák a S. Boriová. Legenda: a – FFI 1; b – FFI 2; c – FFI 3; d – FFI 4; e – FFI 5; f – FFI 6.

Tabela 1. Bodovanie jednotlivých kritérií potrebných pre výpočet fragmentarizačného indexu (FFI; podľa *Outram 2001*, 406). Autorka S. Boriová.

Tabela 2. Zoznam vzoriek analyzovaných oboma mikroskopickými metódami. Autorka S. Boriová.

Tabela 3. Súhrn hlavných znakov pozorovaných pomocou elektrónovej a svetelnej mikroskopie. Autorka S. Boriová.

Translated by Soňa Boriová and Alan K. Outram

Mgr. Soňa Boriová
University of Hradec Králové
Faculty of Arts
Department of Archaeology
Rokitanského 62
CZ – 500 03 Hradec Králové
sona.boriova@uhk.cz

prof. Alan K. Outram
Department of Archaeology
University of Exeter, Laver Building
North Park Road
Exeter EX4 4QE, United Kingdom
A.K.Outram@exeter.ac.uk

Mgr. Zuzana Pokorná, Ph.D.
Czech Academy of Sciences
Institute of Scientific Instruments
Královopolská 147
CZ – 612 64 Brno
zuza@isibrno.cz

doc. Mgr. Sandra Sázelová, Ph.D.
Czech Academy of Sciences
Institute of Archaeology
Research Centre for Paleolithic
and Paleoanthropology Dolní Věstonice
Čechyňská 363/19
CZ – 602 00 Brno
sazelova@arub.cz